Mathematical aspects of vacuum energy on quantum graphs

2009 J. Phys. A: Math. Theor. 42 025204

(http://iopscience.iop.org/1751-8121/42/2/025204)

IOP PUBLISHING JOURNAL OF PHYSICS A: MATHEMATICAL AND THEORETICAL

J. Phys. A: Math. Theor. **42** (2009) 025204 (20pp) doi:10.1088/1751-8113/42/2/025204

Mathematical aspects of vacuum energy on quantum graphs

G Berkolaiko[1], J M Harrison[1,2] and J H Wilson[1,3]

[1] Department of Mathematics, Texas A&M University, College Station, TX 77843-3368, USA
[2] Department of Mathematics, Baylor University, Waco, TX 76798, USA
[3] University of Maryland, Department of Physics, College Park, MD 20742, USA

E-mail: gregory.berkolaiko@math.tamu.edu, jon_harrison@baylor.edu and jwilson.thequark@gmail.com

Received 18 June 2008, in final form 7 October 2008
Published 2 December 2008
Online at stacks.iop.org/JPhysA/42/025204

Abstract

We use quantum graphs as a model to study various mathematical aspects of the vacuum energy, such as convergence of periodic path expansions, consistency among different methods (trace formulae versus method of images) and the possible connection with the underlying classical dynamics. In our study we derive an expansion for the vacuum energy in terms of periodic paths on the graph and prove its convergence and smooth dependence on the bond lengths of the graph. For an important special case of graphs with equal bond lengths, we derive a simpler explicit formula. With minor changes this formula also applies to graphs with rational (up to a common factor) bond lengths. The main results are derived using the trace formula. We also discuss an alternative approach using the method of images and prove that the results are consistent. This may have important consequences for other systems, since the method of images, unlike the trace formula, includes a sum over special 'bounce paths'. We succeed in showing that in our model bounce paths do not contribute to the vacuum energy. Finally, we discuss the proposed possible link between the magnitude of the vacuum energy and the type (chaotic versus integrable) of the underlying classical dynamics. Within a random matrix model we calculate the variance of the vacuum energy over several ensembles and find evidence that the level repulsion leads to suppression of the vacuum energy.

PACS numbers: 03.65.Sq, 05.45.Mt, 03.70.+k, 64.60.aq
Mathematics Subject Classification: 34B45, 81Q10, 15A52

1. Introduction

Vacuum energy is a concept arising in quantum field theory and was first shown by Casimir [1] to have an observable effect on two perfectly conducting parallel plates, causing them to attract. Since then, experiments with various physical geometries have confirmed the effects of vacuum energy (see [2–5]).

In time-independent situations the vacuum energy is formally given by

$$E = \frac{1}{2}\sum_n k_n \tag{1}$$

where k_n^2 are the eigenvalues of a Hamiltonian, H, where throughout we take $\hbar = 1 = c$. The above expression arises in quantum field theory in the context of cavities and cosmological models [3], and it is formally divergent. To get meaningful result from this expression, the vacuum energies for two different configurations are subtracted from one another [2]. To accomplish this in a systematic way, we employ an ultra-violet cutoff defining the energy as the regular part of

$$E(t) = \frac{1}{2}\sum_n k_n \,\mathrm{e}^{-k_n t}, \tag{2}$$

as $t \to 0$. To evaluate (2), it is sometimes convenient to employ the trace of the cylinder kernel, $T(t) = \sum_n \mathrm{e}^{-k_n t}$, [6]. In this way, $E(t) = -T'(t)/2$. The singular term in the expansion of $E(t)$ is related to the vacuum energy density of free space, and physical justification for its removal is described, for example, in [2] (for systems similar to those considered here, see [7, 8]).

A widely employed method of calculation of the vacuum energy is expanding it into a sum over classical paths [9–14]. The expansion is usually done by the method of images, or 'multiple reflections', leading to a sum over all closed paths. It has been argued in [11] that for certain geometries restricting the sum to include only the periodic paths ('semiclassical evaluation') correctly reproduces asymptotic behavior of the vacuum energy and is much simpler to evaluate. A periodic path comes back to the starting point with the same momentum, while a closed path might not. Another popular approximation predicts the sign of the vacuum energy by considering only short orbits [8, 15]. This implicitly assumes that the convergence of the complete series is sufficiently fast.

In the present paper we aim to contribute to this discussion by studying the vacuum energy on quantum graphs (for another model where similar questions are addressed, see [16]). Quantum graphs are often used as mathematical models that exhibit the relevant phenomena while being sufficiently simple to allow mathematical treatment. We compare the method of images with the direct application of the trace formula (which is exact on graphs) and demonstrate that the outcome is the same. This is done by showing that the contribution of the 'bounce paths'—the paths that are closed but not periodic—is identically zero. We also prove that the resulting sums converge, giving an estimate for the rate of convergence, and can be differentiated term by term with respect to the topological parameters present in the model.

One of the main reasons for the success of quantum graphs as models (for example, of quantum chaos, see [17] for a review) is the existence of an exact trace formula on quantum graphs. A trace formula is a relation between the spectrum and the set of periodic orbits of the system. For graphs, the trace formula was first found by Roth [18, 19] and then by Kottos and Smilansky [20]. Subsequent studies of the mathematical properties of the trace formula on graphs included works by Kostrykin, Potthoff and Schrader [21] and Winn [22].

The trace formula of [20] gives an expression for the density of states $d(k)$ defined as

$$d(k) = \sum_{n=1}^{\infty} \delta(k - k_n), \tag{3}$$

where $\delta(\cdot)$ is the Dirac delta function. The vacuum energy is then, formally,

$$E(t) = \frac{1}{2} \int k\, \mathrm{e}^{-kt} d(k)\, \mathrm{d}k, \tag{4}$$

quickly leading to the result (for k-independent scattering matrices, see section 2),

$$E_c = -\frac{1}{2\pi} \sum_{n=1}^{\infty} \sum_{p \in \mathcal{P}_n} \frac{A_p}{n\ell_p}. \tag{5}$$

The inner sum is over the set $\mathcal{P}_n$ of all periodic paths of length n on the graph, ℓ_p is the metric length of the path p and A_p is its stability amplitude (see section 4.1 for definitions).

After introducing the notation in section 2 and considering some explicit examples in section 3, we prove the mathematical correctness of the calculation outlined above. This is done in section 4.3, where the convergence of (5) is also analyzed. In section 4.4 we show that we can differentiate (5) with respect to individual bond lengths, showing the smoothness (C^∞) of E_c as a function of lengths.

In section 5 we briefly discuss the method of images (covered more fully in [23]) and show that the contributions from the bounce paths cancel. Finally, in section 6 we discuss random matrix models of the vacuum energy. As expected, in such models the average vacuum energy is zero and there is no preferred sign to the Casimir force. However, by analyzing the second moment of the energy we confirm an earlier observation by Fulling [6, 24] that the level repulsion tends to decrease the *magnitude* of the energy.

2. Vacuum energy and quantum graphs

Quantum graphs were introduced as a model of the vacuum energy by Fulling [25] who considered the effect of the energy density near a quantum graph vertex by constructing the cylinder kernel for an infinite star graph (a graph with one vertex and B bonds extending to infinity). The quantum field theory origins of this in a graph context were given by Bellazzini and Mintchev [26]. The vacuum energy expression for quantum graphs obtained in the present paper was also used in [8] where the convergence was investigated numerically (we prove rigorous estimates here).

We start by briefly recalling the terminology of the quantum graph model, see [27] for a general review of quantum graphs. We consider a finite metric graph Γ consisting of a set of vertices $\mathcal{V}$, and a set of bonds $\mathcal{B}$. Since the graph is metric, each bond b is associated with a closed interval $[0, L_b]$, thus fixing a preferred direction along the bond (from 0 to L_b). This direction can be chosen arbitrarily. Suppose that for a bond connecting the vertices v and w the direction from v to w is chosen. Then we distinguish three objects, the undirected bond $b = \{v, w\}$ and two directed bonds, $b^+ = (v, w)$ and $b^- = (w, v)$. Whenever the distinction between b^+ and b^- is unimportant, we will denote the directed bonds by Greek letters: α, β. In addition, the reversal of α is denoted by $\bar{\alpha}$ (e.g. if $\alpha = b^+$, then $\bar{\alpha} = b^-$). We will denote by B the number of bonds $|\mathcal{B}|$; correspondingly, the number of directed bonds is $2B$. The length of the directed bond is naturally determined by the length L_b of the underlying undirected bond. The total length of Γ is $\mathcal{L} = \sum_{b \in \mathcal{B}} L_b$. We will denote by $\mathbf{L} = \mathrm{diag}\{L_1, \ldots, L_B, L_1, \ldots, L_B\}$ the diagonal $2B \times 2B$ matrix of directed bond lengths.

In this paper we study the spectrum of the negative Laplacian on the graph. The Laplacian acts on the Hilbert space $\mathcal{H}(\Gamma) := \bigoplus_{b\in\mathcal{B}} H^2([0, L_b])$ of (Sobolev) functions defined on the bonds of the graph. On the bond b it acts as the one-dimensional differential operator $-\frac{\mathrm{d}^2}{\mathrm{d}x_b^2}$. A domain on which the Laplacian is self-adjoint may be defined by specifying matching conditions at the vertices of Γ, see e.g. [27–30].

To specify the matching conditions, let f be a function in $\mathcal{H}(\Gamma)$. For a vertex v of degree d we denote by $\mathbf{f}^{(v)}$ the vector of values of f at v, $\mathbf{f}^{(v)} = \big(f_{b_1}(v), \ldots, f_{b_d}(v)\big)^T$, where $f_b(v) = f_b(0)$ if $b = \{v, w\}$ is oriented from v to w and $f_b(v) = f_b(L_b)$ otherwise. Furthermore, let $\mathbf{g}^{(v)}$ denote the vector of outgoing derivatives of f at v, $\mathbf{g}^{(v)} = \big(f'_{b_1}(v), \ldots, f'_{b_d}(v)\big)^T$, i.e. $f'_b(v) = f'_b(0)$ if $b = \{v, w\}$ is oriented from v to w and $f'_b(v) = -f'_b(L_b)$ otherwise. Matching conditions at v can be specified by a pair of matrices $\mathbb{A}^{(v)}$ and $\mathbb{B}^{(v)}$ through the linear equation

$$\mathbb{A}^{(v)}\mathbf{f}^{(v)} + \mathbb{B}^{(v)}\mathbf{g}^{(v)} = \mathbf{0}. \tag{6}$$

The matching conditions define a self-adjoint operator if $(\mathbb{A}^{(i)}, \mathbb{B}^{(i)})$ has maximal rank and $\mathbb{A}^{(i)}\mathbb{B}^{(i)\dagger}$ is self-adjoint at each vertex (where $\mathbb{B}^{(i)\dagger}$ represents the adjoint of $\mathbb{B}$).

A solution to the eigenvalue equation on the bond b,

$$-\frac{\mathrm{d}^2}{\mathrm{d}x_b^2}\psi_b(x_b) = k^2\psi_b(x_b), \tag{7}$$

can be written as a linear combination of plane waves,

$$\psi_b(x_b) = c_b\,\mathrm{e}^{\mathrm{i}kx_b} + \hat{c}_b\,\mathrm{e}^{-\mathrm{i}kx_b} \tag{8}$$

where c is the coefficient of an outgoing plane wave at 0 and $\hat{c}$ the coefficient of the incoming plane wave at 0. A solution on the whole graph can be defined by specifying the corresponding vector of coefficients $\mathbf{c} = (c_1, \ldots, c_B, \hat{c}_1, \ldots, \hat{c}_B)^T$.

The matching conditions at the vertex v define a vertex scattering matrix

$$\boldsymbol{\sigma}^{(v)}(k) = -(\mathbb{A}^{(v)} + \mathrm{i}k\mathbb{B}^{(v)})^{-1}(\mathbb{A}(v) - \mathrm{i}k\mathbb{B}^{(v)}), \tag{9}$$

see [28]. $\boldsymbol{\sigma}^{(v)}$ is unitary and the elements of $\boldsymbol{\sigma}^{(v)}$ are complex transition amplitudes which in general depend on k. However, for a large class of matching conditions including the so-called Kirchhoff or natural conditions the S-matrix is independent of k. Kirchhoff matching conditions require that ψ is continuous at the vertex and the outgoing derivatives of ψ at the vertex sum to zero. These conditions may be written in the form (6) with matrices

$$\mathbb{A} = \begin{pmatrix} 1 & -1 & 0 & 0 & \ldots \\ 0 & 1 & -1 & 0 & \ldots \\ & & \ddots & \ddots & \\ 0 & \ldots & 0 & 1 & -1 \\ 0 & \ldots & 0 & 0 & 0 \end{pmatrix} \qquad \mathbb{B} = \begin{pmatrix} 0 & 0 & \ldots & 0 \\ \vdots & \vdots & & \vdots \\ 0 & 0 & \ldots & 0 \\ 1 & 1 & \ldots & 1 \end{pmatrix}. \tag{10}$$

Substituting in (9) leads to k-independent transition amplitudes

$$[\boldsymbol{\sigma}]_{ij} = \frac{2}{d} - \delta_{ij}, \tag{11}$$

where d is the degree of v.

The matrix $\boldsymbol{\sigma}^{(v)}$ relates incoming and outgoing plane wave coefficients at v, $\mathbf{c}^{(v)} = \boldsymbol{\sigma}\hat{\mathbf{c}}^{(v)}$. Collecting together transition amplitudes from all the vertices of a graph we may define the familiar $2B \times 2B$ *bond scattering matrix* $\mathbf{S}$ [31] as

$$[\mathbf{S}]_{(v',w')(v,w)} = \delta_{w,v'}[\boldsymbol{\sigma}^{(w)}]_{(v,w')}. \tag{12}$$

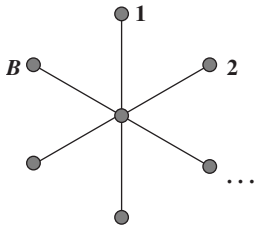

Figure 1. A star graph with B bonds.

We shall also need the *quantum evolution operator* $\mathbf{U} = \mathbf{S}\,\mathrm{e}^{\mathrm{i}k\mathbf{L}}$, which acts on the vector of $2B$ plane wave coefficients indexed by directed bonds. For a general graph, the spectrum can be computed as the zeros of the equation

$$\det(\mathbf{I} - \mathbf{S}\,\mathrm{e}^{\mathrm{i}k\mathbf{L}}) = 0. \tag{13}$$

This formula goes back at least to [32]; for a discussion of scattering matrices of different types we refer the reader to [31].

The following characterization of k-independent bond scattering matrices $\mathbf{S}$ easily follows from the definition of $\mathbf{S}$ and [21, proposition 2.4] applied to the matrices $\boldsymbol{\sigma}^{(v)}$.

Lemma 1. *The* $\mathbf{S}$*-matrix of a graph is* k*-independent if and only if it satisfies*

$$\mathbf{JSJ} = \mathbf{S}^{\dagger}, \tag{14}$$

where $\mathbf{J}$ *is defined by* $J_{\alpha,\beta} = \delta_{\alpha,\bar{\beta}}$ *(*$\bar{\beta}$ *is the reversal of* β*).*

One consequence of (14) is that the solutions of equation (13) are symmetric with respect to 0. This is consistent with k^2 being the eigenvalues of the Hamiltonian.

The spectral theory of quantum graphs is often extended to include quantum evolution operators defined by specifying *a priori* a set of unitary vertex scattering matrices as in [33, 34]. The vertex scattering matrices are typically chosen to be k-independent and to have other desirable features, for instance transition amplitudes of equal magnitude [34, 35]. For such a quantum evolution operator the spectrum is still defined by (13) but, in general, the corresponding scattering matrix $\mathbf{S}$ does not satisfy condition (14) and thus does not come from a self-adjoint Laplace operator on the graph. Still, this model is a valuable tool for exploring statistical properties of the spectrum, in particular its resemblance to the spectrum of large random matrices [17]. We use this model in section 6 to get intuition of the influence of level repulsion on the vacuum energy.

3. Some explicit examples

3.1. Star graph with bonds of equal length

One case where the vacuum energy can be computed explicitly is the quantum star graph with bonds of equal length. This example was first considered in [8] and here, for completeness, we summarize the computation.

Consider a star graph (see figure 1) with B bonds. The bond b has length L_b. We consider the equation (7) with Neumann conditions. At the central vertex, this translates into

$$\sum_b \psi_b'(0) = 0, \qquad \psi_1(0) = \cdots = \psi_B(0) \tag{15}$$

and, at the end-vertices, into

$$\psi_b'(L_b) = 0, \quad \forall\, b. \tag{16}$$

Solutions of (7) together with (16) can be written as

$$\psi_b(x) = C_b \cos(k(L_b - x)).$$

Imposing (15) we conclude that the spectrum consists of the solutions to

$$Z(k) = \sum_{b=1}^{B} \tan(kL_b) = 0,$$

if the lengths are rationally independent. We note that since $Z(k)$ is an increasing function, there is exactly one zero of $Z(k)$ between each pair of consecutive poles. Because of rational independence, the poles of different tangents do not coincide. If we lift the restriction on lengths, in addition to the zeros of $Z(k)$ we have the following eigenvalues: κ is an eigenvalue of multiplicity m if there are $m+1$ lengths L_{b_j} such that κ is a pole of each $\tan(kL_{b_j})$.

In particular, if all lengths are equal, $L_1 = \cdots = L_B = L$, $Z(k)$ is simply $B\tan(kL)$. Each zero of $Z(k)$ is a simple eigenvalue, while each pole is an eigenvalue of multiplicity $B-1$. We can now evaluate

$$T(t) = \sum_{n=1}^{\infty} \mathrm{e}^{-tk_n} = \sum_{n=0}^{\infty} \mathrm{e}^{-n\pi t/L} + (B-1)\sum_{n=0}^{\infty} \mathrm{e}^{-(2n+1)\pi t/2L} = \frac{1+(B-1)\,\mathrm{e}^{-\pi t/2L}}{1-\mathrm{e}^{-\pi t/L}}$$
$$= \frac{BL}{\pi} t^{-1} + \frac{1}{2} - \frac{(B-3)\pi}{24L} t + O(t^2).$$

Now we take the regular part and the limit $t \to 0$ of $-T'(t)/2$ which gives us the vacuum energy

$$E_c = \frac{(B-3)\pi}{48L}. \tag{17}$$

3.2. General graphs with bonds of equal length

If all bond lengths of the graph are equal to L, we can use equation (13) to explicitly describe the infinite spectrum of the graph in terms of the finite spectrum of $\mathbf{S}$. Indeed let $\mathbf{\Lambda}$ be the diagonal matrix of the eigenvalues of $\mathbf{S}$. Then $\mathrm{e}^{\mathrm{i}k\mathbf{L}} = \mathrm{e}^{\mathrm{i}kL}\mathbf{I}$ and, therefore, $\det(\mathbf{I} - \mathbf{S}\,\mathrm{e}^{\mathrm{i}kL\mathbf{I}}) = \det(\mathbf{I} - \mathbf{\Lambda}\,\mathrm{e}^{\mathrm{i}kL})$. Consequently solutions of equation (13) are the values k such that

$$\mathrm{e}^{\mathrm{i}kL}\,\mathrm{e}^{\mathrm{i}\theta_j} = 1, \tag{18}$$

for some j. Here by $\mathrm{e}^{\mathrm{i}\theta_j}$ we denote the jth eigenvalue of (unitary) matrix $\mathbf{S}$. Thus the k-spectrum, the set of *positive* square roots of eigenvalues of the Laplace operator, is given by

$$\bigcup_{j=1}^{2B}\bigcup_{n=1}^{\infty}\left\{\frac{2\pi n - \theta_j}{L}\right\} \tag{19}$$

where we choose θ_j to lie between 0 and 2π. It is important to note that for k-independent matrices $\mathbf{S}$ eigenphases come in pairs, θ_j and $2\pi - \theta_j$, see lemma 1. This ensures that the solutions of (18) occur symmetrically about zero, consistently with the form of equation (7). However, only positive values of k_n are used in the calculation of the vacuum energy, equation (2), hence the restriction $n \geqslant 1$ in (19).

Now we compute the trace of the cylinder kernel $T(t)$

$$T(t) = \sum_{n=1}^{\infty} \mathrm{e}^{-tk_n} = \sum_{j=1}^{2B} \mathrm{e}^{t\theta_j/L} \sum_{n=1}^{\infty} \mathrm{e}^{-2\pi nt/L} = (\mathrm{e}^{2\pi t/L} - 1)^{-1} \sum_{j=1}^{2B} \mathrm{e}^{t\theta_j/L} \tag{20}$$

$$= \sum_{j=1}^{2B} \left[\frac{L}{2\pi t} + \frac{\theta_j - \pi}{2\pi} + \frac{3\theta_j^2 + 2\pi^2 - 6\theta_j\pi}{12L\pi} t + O(t^2) \right]. \tag{21}$$

Thus, the vacuum energy is

$$E_c = -\frac{1}{2} \sum_{j=1}^{2B} \frac{3\theta_j^2 + 2\pi^2 - 6\theta_j\pi}{12L\pi} = -\frac{\pi}{2L} \sum_{j=1}^{2B} B_2(\theta_j/2\pi), \tag{22}$$

where $B_2(\cdot)$ is the second Bernoulli polynomial (compared to the $B = 1$ case discussed in [6]).

As an example of application of formula (22) consider again the star graph with equal bond lengths. The eigenphases θ_j of the S-matrix of a star graph are $0, \pi, \pi/2$ and $3\pi/2$, the latter two with multiplicity $B - 1$. Substituting into equation (22) one can recover (17).

3.3. Graphs with bonds of rational length

By introducing Neumann vertices of degree 2 we do not change the spectrum of the graph and therefore the vacuum energy. On the other hand, if the bonds of the graph are rational (up to an overall factor), by introducing such 'dummy' vertices we can convert the original graph into a graph with bonds of equal length. The number of bonds (and the dimension of the scattering matrix **S**) will increase as a result, but the vacuum energy will still be explicitly computable using equation (22).

Moreover, one can conceivably approximate rationally independent lengths by rational ones and use the result as a numerical approximation to the true vacuum energy. For this approach to work one needs to know, *a priori*, that E_c is continuous as a function of bond lengths. This question is one of the main subjects of section 4.

4. Vacuum energy via the trace formula

4.1. Formal calculation

In this section we perform a formal calculation of the vacuum energy E_c using the trace formula. We shall investigate the rigor of the manipulations in section 4.3.

The trace formula (see, e.g., [17]) connects the spectrum $\{k_n\}$ of the graph with the set of all periodic orbits (or periodic paths) on the graphs. A periodic path of period n is a sequence $(\alpha_1, \alpha_2, \ldots, \alpha_n)$ of directed bonds which satisfy $[\mathbf{S}]_{\alpha_{j+1},\alpha_j} \neq 0$ for all $j = 1, \ldots, n$ (the index $j + 1$ is taken modulo n). A periodic orbit is an equivalence class of periodic paths with respect to the cyclic shift $(\alpha_1, \alpha_2, \ldots, \alpha_n) \mapsto (\alpha_2, \ldots, \alpha_n, \alpha_1)$. We denote by $\mathcal{P}_n$ the set of all periodic paths of period n and by $\mathcal{P}$ the set of periodic paths of all periods. The trace formula can be written as

$$d(k) \equiv \sum_{n=1}^{\infty} \delta(k - k_n) = \frac{\mathcal{L}}{\pi} + \frac{1}{\pi} \mathrm{Re} \sum_{p \in \mathcal{P}} A_p \frac{\ell_p}{n_p} \mathrm{e}^{\mathrm{i}k\ell_p}, \tag{23}$$

where $\mathcal{L}$ is the total length of the graph (the sum of the bond lengths), n_p is the period of the periodic path p, $\ell_p = \sum_{j=1}^{n_p} L_{\alpha_j}$ is the length of p and $A_p = \prod_{j=1}^{n} [\mathbf{S}]_{\alpha_{j+1},\alpha_j}$ is its amplitude. Using the trace formula and equation (2) we can formally compute the vacuum energy. Indeed,

$$\sum_{n=1}^{\infty} k_n \, \mathrm{e}^{-tk_n} = \int_0^{\infty} k \, \mathrm{e}^{-kt} d(k) \, \mathrm{d}k \tag{24}$$

$$= \frac{\mathcal{L}}{2\pi} \int_0^{\infty} k \, \mathrm{e}^{-kt} \, \mathrm{d}k + \frac{1}{\pi} \mathrm{Re} \sum_{p \in \mathcal{P}} A_p \frac{\ell_p}{n_p} \int_0^{\infty} k \, \mathrm{e}^{-kt + \mathrm{i}k\ell_p} \, \mathrm{d}k \tag{25}$$

$$= \frac{\mathcal{L}}{\pi} t^{-2} + \frac{1}{\pi} \mathrm{Re} \sum_{p \in \mathcal{P}} \frac{A_p \ell_p}{n_p (t - \mathrm{i}\ell_p)^2}. \tag{26}$$

Removing the divergent Weyl term $\mathcal{L}/\pi t^2$ due to regularization and taking the limit $t \to 0$ leads to the following simple expression for the vacuum energy:

$$E_c = -\frac{1}{2\pi} \mathrm{Re} \sum_{p \in \mathcal{P}} \frac{A_p}{\ell_p n_p}. \tag{27}$$

4.2. Equal bond lengths; equivalence to (22)

In the case of equal bond lengths (27) should be equivalent to the sum of second Bernoulli polynomials (22). If the length of each bond is L an orbit that visits n bonds has length nL and we may rewrite (27) as a sum over the topological length n followed by a sum over the set of all periodic paths visiting n bonds, $\mathcal{P}_n$,

$$E_c = -\frac{1}{2\pi L} \mathrm{Re} \sum_{n=1}^{\infty} \frac{1}{n^2} \sum_{p \in \mathcal{P}_n} A_p \tag{28}$$

$$= -\frac{1}{2\pi L} \sum_{n=1}^{\infty} \frac{1}{n^2} \sum_{\alpha_1=1}^{2B} \cdots \sum_{\alpha_n=1}^{2B} \mathrm{Re}(S_{\alpha_1\alpha_2} S_{\alpha_2\alpha_3} \ldots S_{\alpha_n\alpha_1}) \tag{29}$$

$$= -\frac{1}{2\pi L} \sum_{n=1}^{\infty} \frac{1}{2n^2} (\mathrm{tr}\, \mathbf{S}^n + \mathrm{tr}(\mathbf{S}^{\dagger})^n) \tag{30}$$

$$= -\frac{1}{2\pi L} \sum_{n=1}^{\infty} \sum_{j=1}^{2B} \frac{\cos n\theta_j}{n^2}, \tag{31}$$

where $\mathrm{e}^{\mathrm{i}\theta_j}$ are the eigenvalues of the matrix $\mathbf{S}$ with $0 \leqslant \theta \leqslant 2\pi$. The sum over n can be expressed in a closed form, see Abramowitz and Stegun [36], formulae 27.8.6,

$$\sum_{n=1}^{\infty} \frac{\cos(n\theta)}{n^2} = \frac{3\theta^2 + 2\pi^2 - 6\pi\theta}{12} = \pi^2 B_2(\theta/2\pi), \tag{32}$$

where $B_2(\cdot)$ is the second Bernoulli polynomial. Consequently we recover expression (22).

4.3. Convergence of (27); vacuum energy as a function of the bond lengths

We shall now present a rigorous derivation of equation (27).

Theorem 1. *The vacuum energy of the graph, defined as*

$$E_c = \frac{1}{2}\lim_{t\to 0+}\left[\sum_{n=1}^{\infty} k_n \,\mathrm{e}^{-tk_n} - \frac{\mathcal{L}}{\pi t^2}\right],$$

is given by

$$E_c = \frac{1}{2\pi}\sum_{n=1}^{\infty}\frac{1}{n}\,\mathrm{Re}\int_0^{\infty}\mathrm{tr}(\mathbf{S}\,\mathrm{e}^{-s\mathbf{L}})^n\,\mathrm{d}s \tag{33}$$

$$= -\frac{1}{2\pi}\,\mathrm{Re}\sum_{n=1}^{\infty}\sum_{p\in\mathcal{P}_n}\frac{A_p}{n\ell_p}, \tag{34}$$

where $\mathcal{P}_n$ denotes the set of all periodic paths of period n. The vacuum energy is smooth (C^∞) as a function of bond lengths on the set $\{L_b > 0\}$.

Remark 1. The sum over the periodic orbits in (34) is finite for each n. We will show, in particular, that the sum over n is absolutely and uniformly convergent. More precisely we will derive the following bound:

$$\left|\sum_{p\in\mathcal{P}_n}\frac{A_p}{\ell_p n}\right| \leqslant \frac{2B}{n^2 L_{\min}}, \tag{35}$$

where $2B$ is the number of (directed) bonds and $L_{\min}$ is the minimal bond length. This estimate shows that, if the (finite!) sum over periodic orbits of a fixed length is performed first, the series in (34) becomes absolutely convergent. Moreover, it is uniformly convergent with respect to the change in bond length as long as $L_{\min}$ remains bounded away from zero.

We would like to mention that our estimate (35) agrees with the numerical results of [8], even though in [8] the ordering of the periodic orbits was different (according to the metric length ℓ_p rather than topological length n).

Proof of (33)–(34). The C^∞ part of the proof will be given in the following section.

We start with the definition of the vacuum energy and integrate by parts

$$\sum_{n=1}^{\infty} k_n\,\mathrm{e}^{-tk_n} = \int_0^{\infty}(tk-1)\,\mathrm{e}^{-tk}N(k)\,\mathrm{d}k, \tag{36}$$

where $N(k)$ is the *integrated density of states* (IDS), a piecewise constant, increasing function

$$N(k) = \#\{n : 0 < k_n < k\}. \tag{37}$$

The integrated density of states $N(k)$ can be split into two parts,

$$N(k) = \mathrm{const} + \frac{k\mathcal{L}}{\pi} + N^{\mathrm{osc}}(k). \tag{38}$$

The first two terms are unimportant: the first term makes no contribution in the integral, and the second term is removed at the regularization stage. The oscillatory part possesses an expansion, see [17], equation (5.24),

$$N^{\mathrm{osc}}(k+\mathrm{i}\varepsilon) = \frac{1}{\pi}\,\mathrm{Im}\sum_{n=1}^{\infty}\frac{1}{n}\,\mathrm{tr}\,\mathbf{U}^n(k+\mathrm{i}\varepsilon), \tag{39}$$

where $\mathbf{U} = \mathbf{S}\,\mathrm{e}^{\mathrm{i}k\mathbf{L}}$.

This expansion is absolutely convergent as long as $\varepsilon > 0$ since the matrix $\mathbf{U}^n(k + \mathrm{i}\varepsilon)$ is then sub-unitary (all eigenvalues lie within a circle of radius strictly less than 1). As $\varepsilon \to 0$, $N^{\mathrm{osc}}(k + \mathrm{i}\varepsilon)$ converges to $N^{\mathrm{osc}}(k)$ pointwise almost everywhere. Moreover, $|N^{\mathrm{osc}}(k + \mathrm{i}\varepsilon)|$ is uniformly bounded by the number of bonds B (in other systems one can show that the Weyl law implies that $|N^{\mathrm{osc}}(k)| = O(k^d)$ as $k \to \infty$ where d is the dimension of the system). Therefore,

$$E_c = -\frac{1}{2} \lim_{t\to 0} \lim_{\varepsilon \to 0} \int_0^\infty (tk - 1)\, \mathrm{e}^{-tk} N^{\mathrm{osc}}(k + \mathrm{i}\varepsilon)\, \mathrm{d}k, \tag{40}$$

and, using the convergence of expansion (39),

$$E_c = -\frac{1}{2\pi} \lim_{t\to 0} \lim_{\varepsilon \to 0} \sum_{n=1}^\infty \frac{1}{n} \operatorname{Im} \int_0^\infty (tk - 1)\, \mathrm{e}^{-tk} [\operatorname{tr} \mathbf{U}^n(k + \mathrm{i}\varepsilon)]\, \mathrm{d}k. \tag{41}$$

We will now show that the integral

$$R_n = \int_0^\infty (tk - 1)\, \mathrm{e}^{-tk} [\operatorname{tr} \mathbf{U}^n(k + \mathrm{i}\varepsilon)]\, \mathrm{d}k \tag{42}$$

is absolutely bounded by $1/n$. Thus the series is absolutely convergent uniformly in ε and t and we can take the limits inside the sum.

A typical term in the (finite!) expansion of the trace is $A_p\, \mathrm{e}^{\mathrm{i}k\ell_p}\, \mathrm{e}^{-\varepsilon\ell_p}$. The two exponential factors, e^{-tk} and $\mathrm{e}^{\mathrm{i}k\ell_p}$ ensure that the integrand is exponentially decaying in k in the first quadrant of $\mathbb{C}$. Therefore we can rotate the contour of integration to the imaginary line, $k = \mathrm{i}s$. The integral becomes

$$R_n = \mathrm{i} \int_0^\infty (\mathrm{i}st - 1)\, \mathrm{e}^{-\mathrm{i}st} \operatorname{tr}(\mathbf{S}\, \mathrm{e}^{-(s+\varepsilon)\mathbf{L}})^n\, \mathrm{d}s. \tag{43}$$

To estimate the trace we apply a version of the Weyl's singular values inequalities [37],

$$|\operatorname{tr} \mathbf{A}^n| \leqslant \operatorname{tr}(\mathbf{A}^\dagger \mathbf{A})^{n/2}, \qquad n \in \mathbb{N} \tag{44}$$

to the matrix $\mathbf{A} = \mathbf{S}\, \mathrm{e}^{-(s+\varepsilon)\mathbf{L}}$. We obtain

$$|\operatorname{tr}\langle \mathbf{S}\, \mathrm{e}^{-(s+\varepsilon)\mathbf{L}})^n| \leqslant \operatorname{tr}\left((\mathbf{S}\, \mathrm{e}^{-(s+\epsilon)\mathbf{L}})^\dagger (\mathbf{S}\, \mathrm{e}^{-(s+\epsilon)\mathbf{L}})\right)^{n/2} = \operatorname{tr}(\mathrm{e}^{-n(s+\epsilon)\mathbf{L}}) \leqslant 2B\, \mathrm{e}^{-nsL_{\min}}, \tag{45}$$

where we used the unitarity of $\mathbf{S}$ and the fact that the $2B$-dimensional matrix $\mathrm{e}^{-(s+\epsilon)\mathbf{L}}$ is diagonal. By $L_{\min}$ we denoted the smallest bond length of the graph. Finally, we can estimate

$$|R_n| \leqslant 2B \int_0^\infty |\mathrm{i}st - 1|\, \mathrm{e}^{-nsL_{\min}}\, \mathrm{d}s \sim \frac{1}{n}. \tag{46}$$

We note that the integrand of (43) can be absolutely bounded by $\mathrm{e}^{-ns(L_{\min}-\delta)}$ for arbitrarily small δ and sufficiently small t. Thus, having brought the limits inside the sum, we can use the dominated convergence theorem to bring them inside the integral. Taking the limit $t \to 0$ and $\varepsilon \to 0$ inside integral (43) produces

$$E_c = \frac{1}{2\pi} \sum_{n=1}^\infty \frac{1}{n} \operatorname{Re} \int_0^\infty \operatorname{tr}(\mathbf{S}\, \mathrm{e}^{-s\mathbf{L}})^n\, \mathrm{d}s. \tag{47}$$

Now we expand the trace,

$$\operatorname{tr}(\mathbf{S}\, \mathrm{e}^{-s\mathbf{L}})^n = \sum_{p \in \mathcal{P}_n} A_p\, \mathrm{e}^{-s\ell_p}, \tag{48}$$

and integrate term by term to recover (34). □

Remark 2. The basic idea of the proof, shifting the convergence into the sub-unitary matrix (see equation (43) and (45)) can also be used to study the convergence of the trace formula itself. This was done in [38].

Remark 3. Since $\mathbf{S}$ is k-independent, the trace in the integral is real and we do not need to take the real part in equations (33)–(34). Indeed, according to lemma 1, the complex conjugate of $\mathrm{tr}(\mathbf{S}\,\mathrm{e}^{-s\mathbf{L}})^n$ is

$$\mathrm{tr}(\mathrm{e}^{-s\mathbf{L}}\mathbf{S}^\dagger)^n = \mathrm{tr}(\mathrm{e}^{-s\mathbf{L}}\mathbf{J}\mathbf{S}\mathbf{J})^n = \mathrm{tr}(\mathbf{S}\mathbf{J}\,\mathrm{e}^{-s\mathbf{L}}\mathbf{J})^n = \mathrm{tr}(\mathbf{S}\,\mathrm{e}^{-s\mathbf{L}})^n, \tag{49}$$

where we used the fact that the length of a bond is invariant with respect to direction reversal and, therefore, $\mathbf{J}\,\mathrm{e}^{-s\mathbf{L}}\mathbf{J} = \mathrm{e}^{-s\mathbf{L}}$.

4.4. Derivatives of the vacuum energy

Proof of differentiability of E_c. We differentiate the expression (33) term by term and show that the result is also absolutely convergent. This can be done by using the following bound on the partial derivatives of $\mathrm{tr}(\mathbf{S}\,\mathrm{e}^{-s\mathbf{L}})^n$:

$$\left|\frac{\partial^{m_1}\dots\partial^{m_B}}{\partial L_1^{m_1}\dots\partial L_B^{m_B}}\,\mathrm{tr}(\mathbf{S}\,\mathrm{e}^{-s\mathbf{L}})^n\right| \leqslant \frac{2B\,\mathrm{e}^{-snL_{\min}/2}}{(L_{\min}/2)^{|\mathbf{m}|}}. \tag{50}$$

Before proving (50) we note that it implies the following bound:

$$\left|\frac{1}{n}\int_0^\infty \frac{\partial^{m_1}\dots\partial^{m_B}}{\partial L_1^{m_1}\dots\partial L_B^{m_B}}\,\mathrm{tr}(\mathbf{S}\,\mathrm{e}^{-s\mathbf{L}})^n\mathrm{d}s\right| \leqslant \frac{2B}{n^2(L_{\min}/2)^{|\mathbf{m}|+1}}. \tag{51}$$

Consequently,

$$\sum_{n=1}^\infty \frac{1}{n}\int_0^\infty \frac{\partial^{m_1}\dots\partial^{m_B}}{\partial L_1^{m_1}\dots\partial L_B^{m_B}}\,\mathrm{tr}(\mathbf{S}\,\mathrm{e}^{-s\mathbf{L}})^n\,\mathrm{d}s$$

converges absolutely and we are therefore allowed to differentiate (33) term by term. We conclude that the vacuum energy is C^∞ as a function of bond lengths.

To prove bound (50) we use the Cauchy integral formula

$$\frac{\partial^{m_1}\dots\partial^{m_B}}{\partial L_1^{m_1}\dots\partial L_B^{m_B}}\,\mathrm{tr}(\mathbf{S}\,\mathrm{e}^{-s\mathbf{L}})^n = \frac{1}{(2\pi)^B}\int_0^{2\pi}\dots\int_0^{2\pi}\frac{\mathrm{tr}(\mathbf{S}\,\mathrm{e}^{-s(\mathbf{L}+\mathbf{R}(\phi))})^n}{R_1^{m_1}\dots R_B^{m_B}}\,\mathrm{d}\phi_1\dots\mathrm{d}\phi_B \tag{52}$$

where $R_j = r_j\mathrm{e}^{\mathrm{i}\phi_j}$ and $\mathbf{R}(\phi) = \mathrm{diag}\{R_1,\dots,R_B,R_1,\dots,R_B\}$. We use (44) again to estimate the trace

$$|\mathrm{tr}(\mathbf{S}\,\mathrm{e}^{-s(\mathbf{L}+\mathbf{R}(\phi))})^n| \leqslant \mathrm{tr}(\mathrm{e}^{-ns(2\mathbf{L}+\mathbf{R}+\mathbf{R}^\dagger)/2}) \leqslant 2B\max_{b=1\dots B}\mathrm{e}^{-s(L_b+r_b\cos(\phi_b))}. \tag{53}$$

By choosing the radius $r_b = L_{\min}/2$ we obtain

$$|\mathrm{tr}(\mathbf{S}\,\mathrm{e}^{-s(\mathbf{L}+\mathbf{R}(\phi))})^n| \leqslant 2B\,\mathrm{e}^{-snL_{\min}/2}. \tag{54}$$

Using this bound in (52) gives

$$\left|\frac{\partial^{m_1}\dots\partial^{m_B}}{\partial L_1^{m_1}\dots\partial L_B^{m_B}}\,\mathrm{tr}(\mathbf{S}\,\mathrm{e}^{-s\mathbf{L}})^n\right| \leqslant \frac{1}{(2\pi)^B}\int_0^{2\pi}\dots\int_0^{2\pi}\frac{2B\,\mathrm{e}^{-snL_{\min}/2}}{(L_{\min}/2)^{|\mathbf{m}|}}\,\mathrm{d}\phi_1\dots\mathrm{d}\phi_B \tag{55}$$

which establishes (50). □

5. Method of images expansion and the equivalence of two expansions

We can evaluate the trace of the cylinder kernel $T(t)$ by constructing the kernel itself. The cylinder kernel, $T_{bb'}(t; x, y)$ where x is measured on bond b and y on bond b' satisfies the following equation on each bond b

$$-\frac{\partial^2}{\partial x^2} T_{bb'}(t; x, y) = \frac{\partial^2}{\partial t^2} T_{bb'}(t; x, y) \tag{56}$$

for $t > 0$, $T_{bb'} \to 0$ as $t \to \infty$, with boundary conditions (6) with respect to the x coordinate, and the initial condition $T_{bb'}(0; x, y) = \delta_{bb'}\delta(x - y)$. By separating variables in (56) it can be shown that the trace of T is

$$T(t) \stackrel{\text{def}}{=} \sum_{b=1}^{B} \int_0^{L_b} T_{bb'}(t; x, x)\, \mathrm{d}x = \sum_n \mathrm{e}^{-k_n t}. \tag{57}$$

The corresponding free space kernel (i.e. the solution of equation (56) on the whole real line with the initial condition $T_0(0; x - y) = \delta(x - y)$) is

$$T_0(t; x - y) = \frac{t/\pi}{t^2 + (x - y)^2}. \tag{58}$$

We can apply the method of images (i.e. multiple reflection) to the free space kernel to obtain the kernel on the graph. The cylinder kernel is then written in terms of paths which begin at y on the bond b' and end at x on the bond b (the details of the construction are given in [23]),

$$\begin{aligned} T_{bb'}(t; x, y) = \delta_{bb'} T_0(t; x - y) + \sum_{n=0}^{\infty} \sum_{\mathbf{p} \in \mathbb{P}_n} [& A_{b^+\mathbf{p}b'^+} T_0(t; L_b + \ell_{\mathbf{p}} + x - y) \\ & + A_{b^+\mathbf{p}b'^-} T_0(t; -\ell_{\mathbf{p}} - x - y) + A_{b^-\mathbf{p}b'^-} T_0(t; -\ell_{\mathbf{p}} - L_b + x - y) \\ & + A_{b^-\mathbf{p}b'^+} T_0(t; L_{b'} + \ell_{\mathbf{p}} + L_b - x - y)]. \end{aligned} \tag{59}$$

In the above expression, we denote the two directed bonds associated with the undirected bond b by b^+ and b^-. The path of topological length n, $\mathbf{p} = (\alpha_1, \ldots, \alpha_n)$ is an n vector of directed bonds and $\mathbb{P}_n$ is the set of all such paths. The metric length of a path is $\ell_{\mathbf{p}} = \sum_{j=1}^{n} L_{\alpha_j}$ and $A_{\mathbf{p}} = [\mathbf{S}]_{\alpha_n \alpha_{n-1}} \cdots [\mathbf{S}]_{\alpha_3 \alpha_2} [\mathbf{S}]_{\alpha_2 \alpha_1}$ is the stability amplitude of the path. Note that even at the stage represented in (59) we have assumed the matrix $\mathbf{S}$ is k-independent.

To obtain the trace, we let $b = b'$ and $y = x$. While this corresponds to 'closing' the paths, we do not always get periodic paths in the topological sense of section 4.1. Indeed, a periodic path would return to the initial point x_b with the same momentum (or direction), whereas when the paths corresponding to the second and fourth terms of (59) return to x_b, the momentum has the opposite sign, see figure 2. The latter paths we shall call *bounce paths*. The difficulty in the method of images is in the handling of the bounce paths.

After integrating $T_{bb}(t; x, x)$ we break the formula into three parts

$$T(t) = T_{\mathrm{FS}}(t) + T_{\mathrm{PO}}(t) + T_{\mathrm{BP}}(t), \tag{60}$$

where FS stands for free space, BP for bounce paths and PO for periodic orbits. The three parts are (taking into account that $T_0(t; x)$ is even in x)

$$T_{\mathrm{FS}}(t) = \sum_{b=1}^{B} \int_0^{L_b} T_0(t; 0)\, \mathrm{d}x = T_0(t; 0)\mathcal{L}, \tag{61}$$

$$T_{\mathrm{PO}}(t) = \sum_{b=1}^{B} \int_0^{L_b} \sum_{n=0}^{\infty} \sum_{\mathbf{p} \in \mathbb{P}_n} [A_{b^+\mathbf{p}b^+} T_0(t; L_b + \ell_{\mathbf{p}}) + A_{b^-\mathbf{p}b^-} T_0(t; \ell_{\mathbf{p}} + L_b)]\, \mathrm{d}x, \tag{62}$$

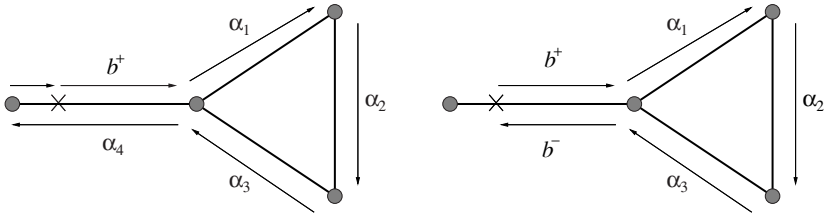

Figure 2. An example of a periodic path (left) and a bounce path (right).

$$T_{\mathrm{BP}}(t) = \sum_{b=1}^{B} \int_0^{L_b} \sum_{n=0}^{\infty} \sum_{\mathbf{p}\in\mathbb{P}_n} [A_{b^+\mathbf{p}b^-} T_0(t;\, \ell_{\mathbf{p}} + 2x) + A_{b^-\mathbf{p}b^+} T_0(t;\, 2L_b + \ell_{\mathbf{p}} - 2x)]\, \mathrm{d}x. \tag{63}$$

We shall use the following lemma to simplify the bounce path term.

Lemma 2. *If the scattering matrix* **S** *of a graph is k-independent, then*

$$\sum_{\alpha=1}^{2B} A_{\alpha\alpha_{n-1}\cdots\alpha_1\bar{\alpha}} = J_{\alpha_1\alpha_{n-1}} A_{\alpha_{n-1}\cdots\alpha_1},$$

where $J_{\alpha,\beta} = \delta_{\alpha,\bar{\beta}}$.

Proof. Writing out the above,

$$\sum_{\alpha} A_{\alpha\alpha_{n-1}\cdots\alpha_1\bar{\alpha}} = S_{\alpha_{n-1}\alpha_{n-2}} \cdots S_{\alpha_3\alpha_2} S_{\alpha_2\alpha_1} \sum_{\alpha} S_{\alpha_1\bar{\alpha}} S_{\alpha\alpha_{n-1}}. \tag{64}$$

The last sum in the above is equivalent to an element of **SJS**, but **JSJS** = **I**, see lemma 1, and $\mathbf{J}^{-1} = \mathbf{J}$, therefore **SJS** = **J**. □

Now we come to the following theorem which proves the equivalence of this method to the trace formula method of section 4.

Theorem 2.

$$T(t) = \frac{\mathcal{L}}{\pi t} + \frac{1}{4}\operatorname{tr}(JS) + \sum_{n=1}^{\infty} \sum_{p\in\mathcal{P}_n} A_p \frac{\ell_p}{n} \frac{t/\pi}{t^2 + \ell_p^2} \tag{65}$$

and consequently,

$$E_c = -\frac{1}{2\pi} \sum_{n=1}^{\infty} \sum_{p\in\mathcal{P}_n} \frac{A_p}{\ell_p n}. \tag{66}$$

Remark 4. A special case of this proof was done for the heat kernel with Kirchhoff conditions by Roth [18, 19]. Similarly, Kostrykin and Schrader have an analog of this proof (again, for the heat kernel) in [21].

Proof. The first term in $T(t)$ is the free space term T_{FS}, which we found above to be equal to $T_0(t;0)\mathcal{L} = \mathcal{L}/\pi t$. Thus we need only consider the periodic path and bounce path terms. *Periodic orbit contribution.* There is no x-dependence in (62), so the integration gives

$$T_{\mathrm{PO}}(t) = \sum_{n=0}^{\infty} \sum_{\mathbf{p}\in\mathbb{P}_n} \sum_{b=1}^{B} [A_{b^-\mathbf{p}b^-} + A_{b^+\mathbf{p}b^+}] T_0(t;\, \ell_{\mathbf{p}} + L_b) L_b. \tag{67}$$

The two amplitudes can be written as a single sum over the directed bond α,

$$\sum_{b=1}^{B}[A_{b^-\mathbf{p}b^-}+A_{b^+\mathbf{p}b^+}]T_0(t;\ell_{\mathbf{p}}+L_b)L_b=\sum_{\alpha=1}^{2B}A_{\alpha\mathbf{p}\alpha}T_0(t;\ell_{\mathbf{p}}+L_\alpha)L_\alpha. \tag{68}$$

The path $\alpha\mathbf{p}\alpha$ is actually a periodic path of period $n+1$ which we will denote by p. The amplitude of p is $A_p=A_{\alpha\mathbf{p}\alpha}$ and its length is $\ell_p=\ell_{\mathbf{p}}+L_\alpha$. Thus,

$$T_{\mathrm{PO}}(t)=\sum_{n=0}^{\infty}\sum_{p\in\mathcal{P}_{n+1}}A_p\frac{\ell_p}{n+1}T_0(t;\ell_p)=\sum_{n=1}^{\infty}\sum_{p\in\mathcal{P}_n}A_p\frac{\ell_p}{n}T_0(t;\ell_p). \tag{69}$$

Bounce path contribution. We can again combine the two amplitudes and change the variables in the integrals to obtain

$$T_{\mathrm{BP}}(t)=\frac{1}{2}\sum_{n=0}^{\infty}\sum_{\mathbf{p}\in\mathbb{P}_n}\sum_{\alpha=1}^{2B}A_{\alpha\mathbf{p}\bar{\alpha}}\int_{\ell_{\mathbf{p}}}^{\ell_{\mathbf{p}}+2L_\alpha}T_0(t;x)\,\mathrm{d}x. \tag{70}$$

We now fix $y>0$ and introduce the cutoff function

$$H(y-x)=\begin{cases}1 & x\leqslant y\\ 0 & x>y.\end{cases} \tag{71}$$

Instead of $T_0(t;x)$ in the integral, we consider $\hat{T}_y(t;x)=T_0(t;x)H(y-x)$. Since the minimum bond length $L_{\min}$ is greater than zero, taking m large enough we will have $\ell_{\mathbf{p}}>y$ for all paths of topological length $m-1$ or greater. Therefore, for a path $\mathbf{p}$ in $\mathbb{P}_{m-1}$ or in $\mathbb{P}_m$ and any α, we can write

$$\int_{\ell_{\mathbf{p}}}^{\ell_{\mathbf{p}}+2L_\alpha}\hat{T}_y(t;x)\,\mathrm{d}x=\int_{\ell_{\mathbf{p}}}^{y}\hat{T}_y(t;x)\,\mathrm{d}x, \tag{72}$$

since the integrand is identically zero on both intervals of integration. We can also ignore all paths from $\mathbb{P}_n$ with $n>m$.

We can therefore write the bounce path contribution with the given cutoff in the following form:

$$\begin{aligned}\hat{T}_{\mathrm{BP}}(t)=&\frac{1}{2}\sum_{n=0}^{m-2}\sum_{\mathbf{p}\in\mathbb{P}_n}\sum_{\alpha=1}^{2B}A_{\alpha\mathbf{p}\bar{\alpha}}\int_{\ell_{\mathbf{p}}}^{\ell_{\mathbf{p}}+2L_\alpha}\hat{T}_y(t;x)\,\mathrm{d}x\\&+\frac{1}{2}\sum_{\mathbf{p}\in\mathbb{P}_{m-1}}\sum_{\alpha=1}^{2B}A_{\alpha\mathbf{p}\bar{\alpha}}\int_{\ell_{\mathbf{p}}}^{y}\hat{T}_y(t;x)\,\mathrm{d}x+\frac{1}{2}\sum_{\mathbf{p}\in\mathbb{P}_m}\sum_{\alpha=1}^{2B}A_{\alpha\mathbf{p}\bar{\alpha}}\int_{\ell_{\mathbf{p}}}^{y}\hat{T}_y(t;x)\,\mathrm{d}x.\end{aligned} \tag{73}$$

Applying lemma 2 to the last set of sums in (73), we obtain

$$\sum_{\mathbf{p}\in\mathbb{P}_m}\sum_{\alpha=1}^{2B}A_{\alpha\mathbf{p}\bar{\alpha}}\int_{\ell_{\mathbf{p}}}^{y}\hat{T}_y(t;x)\,\mathrm{d}x=\sum_{\mathbf{p}\in\mathbb{P}_{m-2}}\sum_{\beta=1}^{2B}A_{\beta\mathbf{p}\bar{\beta}}\int_{\ell_{\mathbf{p}}+2L_\beta}^{y}\hat{T}_y(t;x)\,\mathrm{d}x. \tag{74}$$

Here the new path is the same as the old path but with the first and the last bond removed and β corresponds to the last bond of the old path.

Now we can take the sum corresponding to $n=m-2$ in (73) and add it to the result of (74),

$$\begin{aligned}&\sum_{\mathbf{p}\in\mathbb{P}_{m-2}}\sum_{\alpha=1}^{2B}A_{\alpha\mathbf{p}\bar{\alpha}}\int_{\ell_{\mathbf{p}}}^{\ell_{\mathbf{p}}+2L_\alpha}\hat{T}_y(t;x)\,\mathrm{d}x+\sum_{\mathbf{p}\in\mathbb{P}_{m-2}}\sum_{\beta=1}^{2B}A_{\beta\mathbf{p}\bar{\beta}}\int_{\ell_{\mathbf{p}}+2L_\beta}^{y}\hat{T}_y(t;x)\,\mathrm{d}x\\&\quad=\sum_{\mathbf{p}\in\mathbb{P}_{m-2}}\sum_{\alpha=1}^{2B}A_{\alpha\mathbf{p}\bar{\alpha}}\int_{\ell_{\mathbf{p}}}^{y}\hat{T}_y(t;x)\,\mathrm{d}x.\end{aligned} \tag{75}$$

Therefore, $\hat{T}_{\mathrm{BP}}(t)$ can be rewritten exactly in the form of (73) but with m reduced by 1. Proceeding by induction, we obtain

$$\hat{T}_{\mathrm{BP}}(t) = \frac{1}{2}\sum_{\alpha}^{2B} A_{\alpha\bar{\alpha}} \int_0^y \hat{T}(t; x, y)\,\mathrm{d}x + \frac{1}{2}\sum_{\alpha=1}^{2B} J_{\alpha\alpha} \int_{L_\alpha}^y \hat{T}(t; x, y)\,\mathrm{d}x. \tag{76}$$

However, $J_{\alpha\alpha} = 0$ and we can take the limit $y \to \infty$ to get back $T_{\mathrm{BP}}(t)$,

$$T_{\mathrm{BP}}(t) = \frac{1}{2}\left[\sum_{\alpha=1}^{2B} (\mathbf{SJ})_{\alpha\alpha}\right] \int_0^\infty T_0(t; x)\mathrm{d}x = \frac{1}{4}\,\mathrm{tr}(\mathbf{SJ}). \tag{77}$$

The significance on this term is explored thoroughly in [39]. Since it is constant it vanishes upon differentiation and thus makes no contribution to the vacuum energy expression. □

The above method can be applied to other integral kernels, and we can also find the vacuum energy density if we look at $-\frac{1}{2}\frac{\partial}{\partial t} T_{bb}(t; x, x)$, see [23].

6. Random matrix models of vacuum energy

It has been observed by Fulling [6, 24] that the level repulsion tends to decrease the magnitude of vacuum energy. A natural conclusion would be that in a chaotic system the vacuum energy should be suppressed. Indeed, the spectrum of a generic quantum system with a chaotic classical counterpart is observed to behave like that of a random matrix, which is referred to as the Bohigas–Giannoni–Schmit conjecture [40]. For a system with time-reversal symmetry the appropriate ensemble of unitary matrices is the circular orthogonal ensemble (COE) while in the absence of time-reversal symmetry it is the circular unitary ensemble (CUE), which is the unitary group $U(N)$ with Haar measure, see [41]. For a system with time-reversal symmetry and half-integer spin the random matrix should be drawn from the circular symplectic ensemble (CSE). The corresponding level repulsion is linear (COE), quadratic (CUE) and quartic (CSE). The eigenvalues of an integrable system, in contrast, experience no level repulsion. In this section we attempt to quantify and model any possible connection between level repulsion and the magnitude of vacuum energy.

The first serious problem is that of comparison: vacuum energy should be suppressed compared to what? One cannot directly compare vacuum energy of a chaotic system to that of an integrable one: such systems would be too different. Thus the right approach seems to be to average the energy over an appropriate ensemble of chaotic/integrable systems.

In such situations it is customary to employ random matrices as models of chaotic systems. This, in turn, leads to a second problem: vacuum energy is not an interesting quantity when the spectrum is finite. Thus, (finite) random matrices do not immediately provide a suitable model.

In this section we use a fusion of random matrices and graph models as a testing ground for the above conjecture. Namely, we study quantum graphs with equal bond lengths but with the scattering matrix $\mathbf{S}$ drawn from an appropriate ensemble of unitary matrices. The advantages are clear: each individual system will have an infinite spectrum, the spectra (in the limit of large graphs) will have the desired statistics and the averaging can be done explicitly.

In drawing $\mathbf{S}$ from a random matrix ensemble we are forced to choose a graph which allows scattering between all the edges, in other words a rose graph where one central vertex connects B loops. Moreover, we are departing from the definition of a quantum graph as described in section 2, since a random matrix $\mathbf{S}$ will not, in general, satisfy condition (14). In doing so we are adopting the 'scattering approach' to the construction of quantum graphs,

see [33, 42, 43], and, in essence, *defining* the spectrum $\{k_n\}$ of the graph to be the positive solutions of the secular equation

$$\det(\mathbf{I} - \mathbf{S}\,\mathrm{e}^{\mathrm{i}k\mathbf{L}}) = 0. \tag{78}$$

Such bold generalizations seem to be intrinsic to any random matrix model. Our model should therefore only be regarded as a way to investigate average properties of vacuum energy when its generating spectrum has the desired random matrix level repulsion and not a mathematical statement regarding any given family of quantum graphs.

Before we proceed, we would like to mention one family of quantum graphs (in the sense of section 2) which is believed to have the desired distribution of k_n or, equivalently, the phases θ_j: the random regular graphs. The spectrum of their discrete Laplacian was investigated numerically in [44] and found to display the random-matrix-like statistics. There is a well-known connection between $\{k_n\}$ for a graph with equal edge lengths and the spectrum of its discrete Laplacian, see [27, 45–47], allowing us to conclude that the statistics of the phases θ_j will also follow the random-matrix prediction. However, a rigorous proof of these observations is a mathematical challenge of a formidable difficulty and lies outside the scope of this work.

6.1. Average vacuum energy

The analysis of sections 3 and 4 applies without any changes to the spectrum $\{k_n\}$ defined by (78) with an arbitrary unitary $\mathbf{S}$. Thus the average vacuum energy of our model can be evaluated using equation (22), which expresses the vacuum energy of a graph with equal bond lengths in terms of the eigenphases of $\mathbf{S}$. Using the standard expression for the eigenphase density of the random matrices results in

$$\langle E_c\rangle_\beta = -\frac{\pi}{2L}\frac{1}{\mathcal{N}_\beta}\int_0^{2\pi}\cdots\int_0^{2\pi}\sum_{j=1}^{2B}B_2(\theta_j/2\pi)\prod_{l<m}\left|2\sin\left(\frac{\theta_l-\theta_m}{2}\right)\right|^\beta \mathrm{d}\theta_1\ldots\mathrm{d}\theta_{2B} = 0 \tag{79}$$

where $\mathcal{N}_\beta$ is a normalization constant and $\beta = 1$ for the COE, $\beta = 2$ for the CUE and $\beta = 4$ for CSE.

The eigenphases of an integrable system, in contrast, behave like uniformly distributed random numbers on the interval $[0, 2\pi]$. This can also be modeled by integrating the vacuum energy expression, equation (22), over $2B$ independent uniform random phases,

$$\langle E_c\rangle_{\text{Poisson}} = -\frac{\pi}{2L}\frac{1}{(2\pi)^{2B}}\int_0^{2\pi}\cdots\int_0^{2\pi}\sum_{j=1}^{2B}B_2(\theta_j/2\pi)\,\mathrm{d}\theta_1\ldots\mathrm{d}\theta_{2B} = 0. \tag{80}$$

In each case the average $\langle E_c\rangle$ of the vacuum energy is zero. In fact, the vacuum energy expression must be zero when averaged over any measure which is invariant under a rotation of all the eigenphases by some angle γ. Indeed, in section 4.2 we have shown that

$$E_c = -\frac{1}{2\pi L}\sum_{n=1}^{\infty}\frac{1}{2n^2}(\operatorname{tr}\mathbf{S}^n + \operatorname{tr}(\mathbf{S}^\dagger)^n). \tag{81}$$

But for any rotationally invariant distribution of eigenphases on the unit circle, $\langle\operatorname{tr}\mathbf{S}^n\rangle = 0$ for all $n > 0$ and thus the mean vacuum energy is always zero. As the Casimir force is the derivative of E_c with respect to L this suggests that there is no *a priori* reason to expect either an attractive or repulsive force based purely on the underlying nature of the classical dynamics.

6.2. Variance

To get a handle on how the magnitude of the vacuum energy is affected by the distribution of the eigenvalues we will calculate the variance of the vacuum energy for the ensembles of random graphs introduced previously. For Poisson distributed eigenphases the variance is

$$\begin{aligned}\langle E_c^2\rangle_{\text{Poisson}} &= \frac{\pi^2}{4L^2}\frac{1}{(2\pi)^{2B}}\int_0^{2\pi}\cdots\int_0^{2\pi}\sum_{j=1}^{2B}B_2^2(\theta_j/2\pi)\,\mathrm{d}\theta_1\ldots\,\mathrm{d}\theta_{2B}\\ &= \frac{\pi^2 B}{360L^2},\end{aligned} \tag{82}$$

where $2B$ is the dimension of $\mathbf{S}$ and we used the independence of θ_j to conclude that

$$\langle B_2(\theta_r/2\pi)B_2(\theta_j/2\pi)\rangle = \langle B_2(\theta_r/2\pi)\rangle\langle B_2(\theta_r/2\pi)\rangle = 0. \tag{83}$$

The variance of the vacuum energy modeled by random matrices from the circular ensembles can be computed using expression (30),

$$\langle E_c^2\rangle = \frac{1}{4\pi^2L^2}\sum_{m,n=1}^{\infty}\frac{1}{4n^2m^2}\langle(\operatorname{tr}\mathbf{S}^n+\operatorname{tr}(\mathbf{S}^\dagger)^n)(\operatorname{tr}\mathbf{S}^m+\operatorname{tr}(\mathbf{S}^\dagger)^m)\rangle. \tag{84}$$

For the circular ensembles $\langle\operatorname{tr}\mathbf{S}^n\operatorname{tr}(\mathbf{S}^\dagger)^m\rangle = 0$ unless $m = n$ as the average of a product of matrix elements is zero unless the number of elements of the matrix and the number from its Hermitian conjugate are the same [48]. Consequently

$$\langle E_c^2\rangle = \frac{1}{8\pi^2L^2}\sum_{n=1}^{\infty}\frac{1}{n^4}\langle|\operatorname{tr}\mathbf{S}^n|^2\rangle. \tag{85}$$

We note that $\langle|\operatorname{tr}\mathbf{S}^n|^2\rangle$ is the form factor of the (finite) ensemble and use the standard formulae [41] for CUE

$$\langle|\operatorname{tr}\mathbf{S}^n|^2\rangle_{\text{CUE}} = \begin{cases}(2B)^2 & n=0\\ n & |n|<2B\\ 2B & |n|\geqslant 2B\end{cases} \tag{86}$$

to obtain

$$\langle E_c^2\rangle_{\text{CUE}} = \frac{1}{8\pi^2L^2}\left(\frac{1}{2}\Psi^{(2)}(2B)+\zeta(3)+\frac{B}{3}\Psi^{(3)}(2B)\right) \tag{87}$$

where $\Psi^{(n)}(x)$ is the nth polygamma function and ζ the Riemann zeta function. For all fixed B this is less than $\pi^2B/360$ the variance of the Poisson distributed eigenphases. In fact

$$\lim_{B\to\infty}\langle E_c^2\rangle_{\text{CUE}} = \frac{\zeta(3)}{8\pi^2L^2}. \tag{88}$$

This result parallels that for a random matrix model of the grand potential considered in [16]. Thus, while the variance of the Poisson ensemble grows linearly with matrix size, the CUE variance converges.

The relevant parts of the form factor of the COE and CSE for finite matrix size are

$$\langle|\operatorname{tr}\mathbf{S}^n|^2\rangle_{\text{COE}} = \begin{cases}2n - n\displaystyle\sum_{m=1}^{n}\frac{1}{m+(2B-1)/2} & 0<n\leqslant 2B,\\ 4B - n\displaystyle\sum_{m=1}^{2B}\frac{1}{m+n-(2B+1)/2} & 2B\leqslant n,\end{cases} \tag{89}$$

$$\langle |\operatorname{tr} \mathbf{S}^n|^2 \rangle_{\mathrm{CSE}} = \begin{cases} 2n + n \displaystyle\sum_{m=1}^{n} \frac{1}{(2B+1)/2 - m} & 0 < n \leqslant 2B, \\ 4B & 2B \leqslant n. \end{cases} \tag{90}$$

Note that in the CSE form factor the double degeneracy of the eigenphases of $\mathbf{S}$ (Kramers' degeneracy) has not been lifted. Using (85) we evaluate

$$\langle E_c^2 \rangle_{\mathrm{COE}} = \frac{1}{4\pi^2 L^2} \left(\left(\frac{1}{2} \Psi^{(2)}(2B) + \zeta(3) \right) \left(1 + \frac{1}{2} \Psi(B + 1/2) \right) - \sum_{n=1}^{2B-1} \frac{\Psi(n + B + 1/2)}{2n^3} + \sum_{n=2B}^{\infty} \left[\frac{2B}{n^4} + \frac{\Psi(n - B + 1/2) - \Psi(n + B - 1/2)}{2n^3} \right] \right), \tag{91}$$

$$\langle E_c^2 \rangle_{\mathrm{CSE}} = \frac{1}{4\pi^2 L^2} \left(\left(\frac{1}{2} \Psi^{(2)}(2B) + \zeta(3) \right) \left(1 + \frac{1}{2} \Psi(1/2 - B) \right) - \sum_{n=1}^{2B-1} \frac{\Psi(n - B + 1/2)}{2n^3} + \frac{B}{3} \Psi^{(3)}(2B) \right). \tag{92}$$

For $B > 1$, $\langle E_c^2 \rangle_{\mathrm{COE}}$ and $\langle E_c^2 \rangle_{\mathrm{CSE}}$ are less than $\langle E_c^2 \rangle_{\mathrm{Poisson}}$.

While the results do not have a simple closed form, in the limit of large matrices the result is rather concise:

$$\lim_{B \to \infty} \langle E_c^2 \rangle_{\mathrm{COE}} = \frac{\zeta(3)}{4\pi^2 L^2} = \lim_{B \to \infty} \langle E_c^2 \rangle_{\mathrm{CSE}}. \tag{93}$$

Modeling the vacuum energy variance of a quantum graph through random matrices suggests that the magnitude of the vacuum energy where eigenphases of $\mathbf{S}$ experience level repulsion are indeed smaller on average than those where the eigenphases are Poisson distributed. Moreover, the magnitude gets smaller as the level repulsion increases from linear (COE) to quadratic (CUE) and quartic (CSE). Indeed, to compare the effect of the increased level repulsion in CSE we need to lift the Kramers' degeneracy: otherwise the degeneracy 'compensates' the repulsion. Without the degeneracy, the result for CSE becomes four times smaller

$$\lim_{B \to \infty} \langle E_c^2 \rangle_{\mathrm{CSE/Kramers}} = \frac{\zeta(3)}{16\pi^2 L^2},$$

thus leading to

$$\langle E_c^2 \rangle_{\mathrm{COE}} > \langle E_c^2 \rangle_{\mathrm{CUE}} > \langle E_c^2 \rangle_{\mathrm{CSE/Kramers}},$$

for $B > 1$.

7. Conclusions

Through both the method of images and the trace formula, we demonstrate that the vacuum energy in quantum graphs is a well-defined quantity (i.e. it is both convergent and a smooth function of the bond lengths). The closed form expression (5) is dependent only on the periodic paths in the quantum graph; this is a consequence of the exactness of the trace formula which includes only those paths. Having demonstrated how the bounce paths (closed paths that are not periodic) cancel when using the method of images we hope that our proof will shed light

on the observation that periodic paths provide the correct leading asymptotic behavior even when the trace formula is only semiclassically correct.

The smoothness of the expression for the vacuum energy in a quantum graph allows us to suggest an alternative method for its calculation, by approximating with systems with simpler geometries. In the case of graphs the 'simpler geometry' means rational bond lengths, where an explicit expression for the vacuum energy is obtained.

We also suggest a random ensemble model for the vacuum energy when the statistics of the spectrum are Poisson (for integrable systems) or random matrix (for chaotic systems). We find the average energy in both cases to be zero, thus giving no *a priori* reason to expect a positive or negative energy from the dynamics. Furthermore, we find the variance of the energy and conclude that the magnitude of the energy is typically smaller when the level repulsion is stronger. We stress that this prediction is only correct in the probabilistic sense and no conclusions about particular systems can yet (if ever!) be drawn.

Acknowledgments

The authors would like to thank S A Fulling, J P Keating, K Kirsten, P Kuchment, M Pivarsky, B Winn and anonymous referees for their helpful comments. This material is based upon work supported by the National Science Foundation under Grants No. DMS-0604859, PHY-0554849 and DMS-0648786. The authors would also like to thank the Isaac Newton Institute for Mathematical Sciences, Cambridge, UK, where part of the research took place.

References

[1] Casimir H B 1948 On the attraction between two perfectly conducting plates *Proc. K. Ned. Akad. Wet.* **51** 793–5
[2] Boyer T H 1970 Quantum zero-point energy and long-range forces *Ann. Phys.* **56** 474–503
[3] Plunien G, Müller B and Greiner W 1986 The Casimir effect *Phys. Rep.* **134** 87–193
[4] Bordag M, Mohideen U and Mostepanenko V M 2001 New developments in the Casimir effect *Phys. Rep.* **353** 1–205
[5] Milton K A 2004 The Casimir effect: recent controversies and progress *J. Phys. A: Math. Gen.* **37** R209–77
[6] Fulling S A 2004 Global and local vacuum energy and closed orbit theory *Proc. of the 6th Workshop on Quantum Field Theory under the Influence of External Conditions (Norman, Oklahoma Sept. 2003)* ed K Milton (Princeton, NJ: Rinton Press) pp 166–74
[7] Cavalcanti R M 2004 Casimir force on a piston *Phys. Rev.* D **69** 065015
[8] Fulling S A, Kaplan L and Wilson J H 2007 Vacuum energy and repulsive Casimir forces in quantum star graphs *Phys. Rev.* A **76** (arXiv:0703248v1)
[9] Brown L S and Maclay G J 1969 Vacuum stress between conducting plates: an image solution *Phys. Rev.* **184** 1272–9
[10] Jaekel M T and Reynaud S 1991 Casimir force between partially transmitting mirrors *J. Physique* I **1** 1395–409
[11] Schaden M and Spruch L 1998 Infinity-free semiclassical evaluation of Casimir effects *Phys. Rev.* A **58** 935–53
[12] Fulling S A 2002 Periodic orbits, spectral oscillations, scaling, and vacuum energy: beyond HaMiDeW *Proc. Int. Meeting on Quantum Gravity and Spectral Geometry, (Naples, 2001) Nucl. Phys.* B (Proc. Suppl.) **104** 161–4
[13] Jaffe R L and Scardicchio A 2004 Casimir effect and geometric optics *Phys. Rev. Lett.* **92** 070402
[14] Liu Z H and Fulling S A 2006 Casimir energy with a Robin boundary: the multiple-reflection cylinder-kernel expansion *New J. Phys.* **8** 234
[15] Martin S 2006 Sign and other aspects of semiclassical Casimir energies *Phys. Rev.* A **73** 042102
[16] Leboeuf P, Monastra A G and Bohigas O 2001 The Riemannium *Regul. Chaotic Dyn.* **6** 205–10
[17] Gnutzmann S and Smilansky U 2006 Quantum graphs: applications to quantum chaos and universal spectral statistics *Adv. Phys.* **55** 527–625
[18] Roth J-P 1984 Le spectre du laplacien sur un graphe *Théorie du potentiel (Orsay, 1983) Lecture Notes in Math.* vol 1096 ed G Mokobodzki and D Pinchon (Berlin: Springer) pp 521–39

[19] Roth J-P 1983 Spectre du laplacien sur un graphe *C. R. Acad. Sci. Paris Sér. I Math.* **296** 793–5
[20] Kottos T and Smilansky U 1997 Quantum chaos on graphs *Phys. Rev. Lett.* **79** 4794–7
[21] Kostrykin V, Potthoff J and Schrader R 2007 Heat kernels on metric graphs and a trace formula *Adventures in Mathematical Physics* ed F Germinet and P D Hislop (*Contemporary mathematics* vol 447) (Providence, RI: American Mathematical Society) pp 175–98
[22] Winn B 2006 On the trace formula for quantum star graphs *Quantum Graphs and their Applications* (*Contemp. Math.* vol 415) ed G Berkolaiko, R Carlson, S Fulling and P Kuchment (Providence, RI: American Mathematical Society) pp 293–307
[23] Wilson J H 2007 Vacuum energy in quantum graphs. *Undergraduate Research Fellow Thesis* Texas A&M University. http://handle.tamu.edu/1969.1/5682
[24] Fulling S A 2003 private communication
[25] Fulling S A 2006 Local spectral density and vacuum energy near a quantum graph vertex *Quantum Graphs and their Applications* (*Contemp. Math.* vol 415) ed G Berkolaiko, R Carlson, S Fulling and P Kuchment (Providence, RI: American Mathematical Society) pp 161–72
[26] Bellazzini B and Mintchev M 2006 Quantum fields on star graphs *J. Phys. A: Math. Gen.* **39** 11101–17
[27] Kuchment P 2004 Quantum graphs. I: some basic structures *Waves Random Media* **14** S107–28
[28] Kostrykin V and Schrader R 1999 Kirchhoff's rule for quantum wires *J. Phys. A: Math. Gen.* **32** 595–630
[29] Kostrykin V and Schrader R 2000 Kirchhoff's rule for quantum wires. II: the inverse problem with possible applications to quantum computers *Fortschr. Phys.* **48** 703–16
[30] Kostrykin V and Schrader R 2001 The generalized star product and the factorization of scattering matrices on graphs *J. Math. Phys.* **42** 1563–98
[31] Kottos T and Smilansky U 1999 Periodic orbit theory and spectral statistics for quantum graphs *Ann. Phys.* **274** 76–124
[32] von Below J 1985 A characteristic equation associated to an eigenvalue problem on c^2-networks *Linear Algebra Appl.* **71** 309–25
[33] Schanz H and Smilansky U 2000 Spectral statistics for quantum graphs: periodic orbits and combinatorics *Proc. of the Australian Summer School on Quantum Chaos and Mesoscopics Phil. Mag.* B **80** 1999–2021.
[34] Tanner G 2001 Unitary stochastic matrix ensembles and spectral statistics *J. Phys. A: Math. Gen.* **34** 8485–500
[35] Harrison J M, Smilansky U and Winn B 2007 Quantum graphs where back-scattering is prohibited *J. Phys. A: Math. Theor.* **40** 14181–93
[36] Abramowitz M and Stegun I A 1964 *Handbook of Mathematical Functions* (New York: Dover)
[37] Weyl H 1949 Inequalities between the two kinds of eigenvalues of a linear transformation *Proc. Nat. Acad. Sci. USA* **35** 408–11
[38] Winn B 2008 A conditionally convergent trace formula for quantum graphs 'Analysis on Graphs and its Applications' *Proc. Symp. in Pure Mathematics* eds P Exner, J P Keating, P Kuchment, T Sunada and A Teplyaev (Providence, RI: Amer. Math. Soc) **77** 491–501
[39] Fulling F, Kuchment P and Wilson J H 2007 Index theorems for quantum graphs *J. Phys. A: Math. Theor.* **40** 14165–80
[40] Bohigas O, Giannoni M and Schmit C 1984 Characterization of chaotic quantum spectra and universality of level fluctuation laws *Phys. Rev. Lett.* **52** 1–4
[41] Haake F 2006 *Quantum Signatures of Chaos* 2nd edn (Berlin: Springer)
[42] Tanner G 2000 Spectral statistics for unitary transfer matrices of binary graphs *J. Phys. A: Math. Gen.* **33** 3567–85
[43] Berkolaiko G 2008 Two constructions of quantum graphs and two types of spectral statistics *Analysis on Graphs and its Applications* ed P Exner, J Keating, P Kuchment, T Sunada and A Teplyaev (Providence, RI: American Mathematical Society) **77** 315–29
[44] Jakobson D, Miller S D, Rivin I and Rudnick Z 1999 Eigenvalue spacings for regular graphs *Emerging applications of number theory (Minneapolis, MN, 1996)* (*IMA Vol. Math. Appl.* vol 109) (New York: Springer) pp 317–327
[45] Alexander S 1985 Superconductivity of networks: a percolation approach to the effects of disorder *Phys. Rev.* B **27** 1541–57
[46] Cattaneo C 1997 The spectrum of the continuous Laplacian on a graph *Monatsh. Math.* **124** 215–35
[47] Exner P 1997 A duality between Schrödinger operators on graphs and certain Jacobi matrices *Ann. Inst. Henri Poincaré Phys. Théor.* **66** 359–71
[48] Brouwer P W and Beenakker C W J 1996 Diagrammatic method of integration over the unitary group, with applications to quantum transport in mesoscopic systems *J. Math. Phys.* **37** 4904–34